PHILOSOPHICAL TRANSACTIONS OF THE ROYAL SOCIETY A MATHEMATICAL, PHYSICAL & ENGINEERING SCIENCES

Photoelectrochemical Cells

A. J. Nozik

Phil. Trans. R. Soc. Lond. A 1980 **295**, 453-470
doi: 10.1098/rsta.1980.0141

Phil. Trans. R. Soc. Lond. A **295**, 453–470 (1980)
Printed in Great Britain

Photoelectrochemical cells

By A. J. Nozik†
Solar Energy Research Institute, Golden, Colorado 80401, *U.S.A.*

The application of photoelectrochemical systems based on photoactive semiconducting electrodes to the problem of solar energy conversion and chemical synthesis is discussed. Three types of cells are described: electrochemical photovoltaic cells (wherein optical energy is converted into electrical energy); photoelectrolysis cells (wherein optical energy is converted into chemical free energy); and photocatalytic cells (wherein optical energy provides the activation energy for exoergic chemical reactions). The critical semiconductor electrode properties for these cells are the band gap, the flat-band potential, and photoelectrochemical stability. No semiconductor electrode material is yet known for which all three parameters are simultaneously optimized. An interesting configurational variation of photoelectrolysis cells, labelled 'photochemical diodes', is described. These diodes comprise cells that have been collapsed into monolithic particles containing no external wires. Recent advances in several areas of photoelectrochemical systems are also described.

1. Introduction

In recent years a great deal of interest has developed in the field of photoelectrochemistry based on photoactive semiconducting electrodes, and especially in the application of these systems to solar energy conversion and chemical synthesis (Fujishima & Honda 1972; Nozik 1978; Gerischer 1977*a*; Bard 1978; Wrighton 1977; Harris & Wilson 1978; Maruska & Ghosh 1978). A general classification scheme for the various types of photoelectrochemical cells is presented in figure 1. The first division is into (*a*) cells wherein the free energy change in the electrolyte is zero (these are labelled electrochemical photovoltaic cells), and (*b*) cells wherein the free energy in the electrolyte is non-zero (these are labelled photoelectrosynthetic cells). In the former cell, only one effective redox couple is present in the electrolyte and the oxidation and reduction reactions at the anode and cathode are inverse to each other. The net photoeffect is the circulation of charge external to the cell, producing an external photovoltage and photocurrent (a liquid junction solar cell); no chemical change occurs in the electrolyte.

In the photoelectrosynthetic cell, two effective redox couples are present in the electrolyte, and a net chemical change occurs upon illumination. If the free energy change of the net electrolyte reaction is positive, optical energy is converted into chemical energy and the process is labelled photoelectrolysis. On the other hand, if the net electrolyte reaction has a negative free energy change, optical energy provides the activation energy for the reaction, and the process is labelled photocatalysis. All three types of photoelectrochemical cells will be reviewed and discussed in this paper.

† Experimental work reported here was done at the Corporate Research Center, Allied Chemical Corporation, Morristown, N.J. 07960, U.S.A.

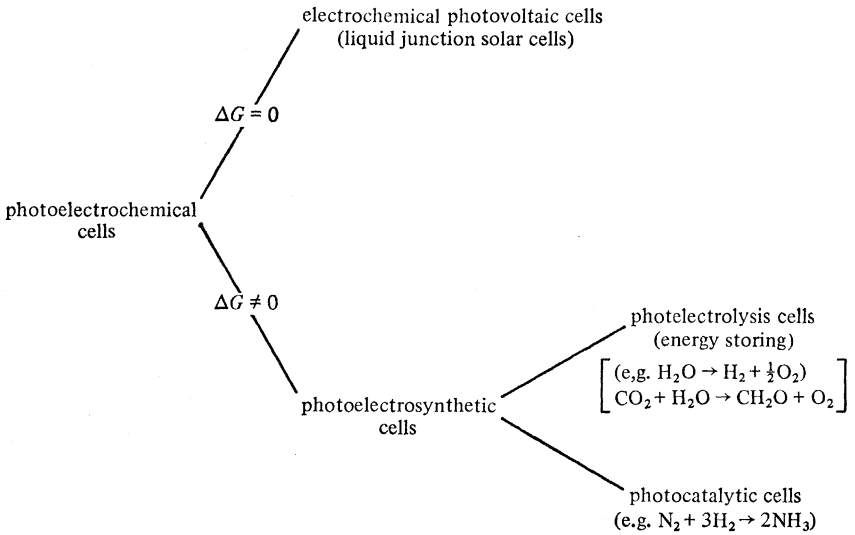

FIGURE 1. Classification scheme for photoelectrochemical cells.

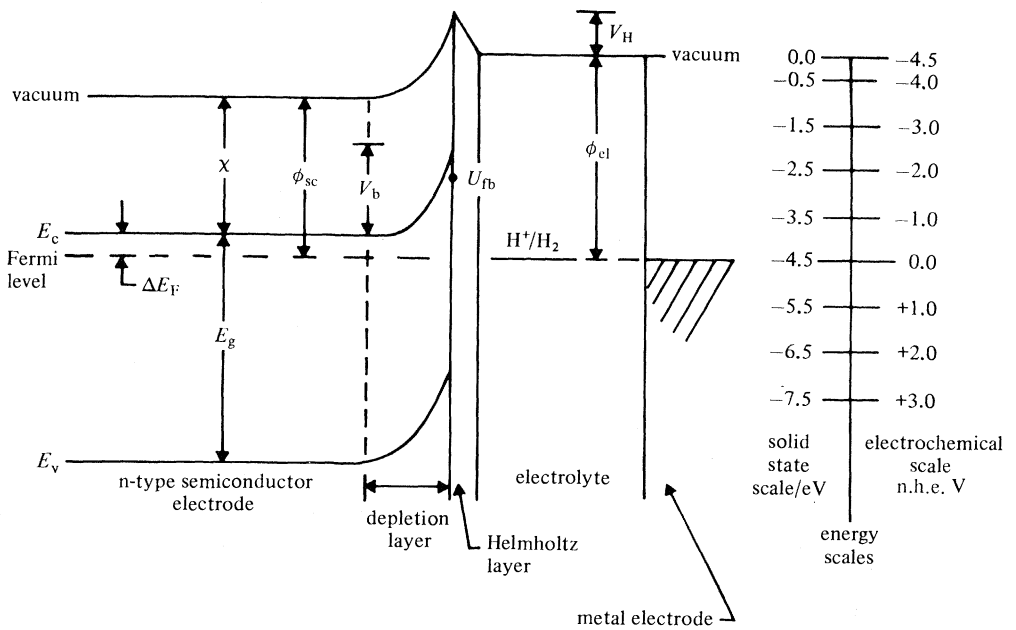

FIGURE 2. Energy level diagram for semiconductor–electrolyte junction showing the relations between the electrolyte redox couple (H^+/H_2), the Helmholtz layer potential drop (V_H), and the semiconductor band gap (E_g), electron affinity (χ), work function (ϕ_{sc}), band bending (V_b), and flat-band potential (V_{fb}). The electrochemical and solid state energy scales are shown for comparisons; ϕ_{el} is the electrolyte work function.

2. SEMICONDUCTOR–ELECTROLYTE JUNCTIONS

All phenomena associated with photoelectrochemical systems are based on the formation of a semiconductor–electrolyte junction when an appropriate semiconductor is immersed in an appropriate electrolyte. The junction is characterized by the presence of a space charge layer in the semiconductor adjacent to the interface with the electrolyte. A space charge layer generally develops in a semiconductor upon contact and equilibration with a second phase

whenever the initial chemical potential of electrons is different for the two phases. For semiconductors, the chemical potential of electrons is given by the Fermi level in the semiconductor. For liquid electrolytes, the chemical potential of electrons is determined by the redox potential of the redox couples present in the electrolyte; these redox potentials are also identified with the Fermi level of the electrolyte.

If the initial Fermi level in an n-type semiconductor is above the initial Fermi level in the electrolyte (or any second phase), then equilibration of the two Fermi levels (or chemical potentials) occurs by transfer of electrons from the semiconductor to the electrolyte. This produces a positive space charge layer in the semiconductor (also called a depletion layer since the region is depleted of majority charge carriers). As a result, the conduction and valence band edges are bent upwards, establishing a potential barrier against further electron transfer into the electrolyte (see figure 2). An inverse but analogous situation occurs with p-type semiconductors having an initial Fermi level below that of the electrolyte.

A charged layer also exists in the electrolyte adjacent to the interface with the solid electrode – the well known Helmholtz layer. This layer consists of charged ions from the electrolyte adsorbed on the solid electrode surface; these ions are of opposite sign to the charge induced in the solid electrode. The width of the Helmholtz layer is generally of the order of a few ångstroms†. The potential drop across the Helmholtz layer depends upon the specific ionic equilibrium obtaining at the surface.

A very important consequence of the presence of the Helmholtz layer for semiconductor electrodes is that it markedly affects the band bending that develops in the semiconductor when it equilibrates with the electrolyte. Without the Helmholtz layer, the band bending would simply be expected to equal the difference in initial Fermi levels between the two phases (i.e. the difference between their respective work functions). However, the potential drop across the Helmholtz layer modifies the net band bending as shown in figure 2. This effect is similar to the well known situation in Schottky junctions formed between semiconductors and metals, where the potential barrier and band bending are usually strongly influenced by the presence of semiconductor surface states.

In figure 2, the energy scales commonly used in solid state physics and in electrochemistry are shown for comparison. In the former, the zero reference point is vacuum, while in the latter it is the standard redox potential of the hydrogen ion-hydrogen (H^+/H_2) redox couple. It has been shown (Gerischer 1975; Lohmann 1967) that the effective work function or Fermi level for the standard (H^+/H_2) redox couple at equilibrium is -4.5 eV with respect to vacuum. Hence, by using this scale factor, the energy levels corresponding to any given redox couple can be related to the energy levels of the valence and conduction bands of the semiconductor electrode.

To make the connection between the energy levels of the electrolyte and the semiconductor it is necessary to introduce the flat-band potential, U_{fb}, as a critical parameter characterizing the semiconductor electrode. The flat-band potential is the electrode potential at which the semiconductor bands are flat (zero space charge in the semiconductor); it is measured with respect to a reference electrode, usually either the standard normal H^+/H_2 redox potential (n.h.e.) or the standard calomel electrode (s.c.e.). Hence, the band bending is given by

$$V_b = U_e - U_{fb}, \tag{1}$$

† 1 Å $= 10^{-1}$ nm $= 10^{-10}$ m.

PHILOSOPHICAL TRANSACTIONS OF THE ROYAL SOCIETY A MATHEMATICAL, PHYSICAL & ENGINEERING SCIENCES

where U_e is the electrode potential (Fermi level) of the semiconductor. At equilibrium in the dark, U_e is identical with the potential of the redox couple in the electrolyte.

The effect of the Helmholtz layer on the semiconductor band bending is contained within the flat-band potential. This important parameter is a property both of the semiconductor bulk and the electrolyte, as seen from the following relation:

$$U_{fb}\,(\text{n.h.e.}) = (\chi + \Delta E_F + V_H) - 4.5 = (\phi_{sc} + V_H) - 4.5, \tag{2}$$

where χ is the electron affinity of the semiconductor, ϕ_{sc} is the work function of the semiconductor, ΔE_F is the difference between the Fermi level and majority carrier band edge of the semiconductor, V_H is the potential drop across the Helmholtz layer, and 4.5 is the scale factor relating the H^+/H_2 redox level to vacuum.

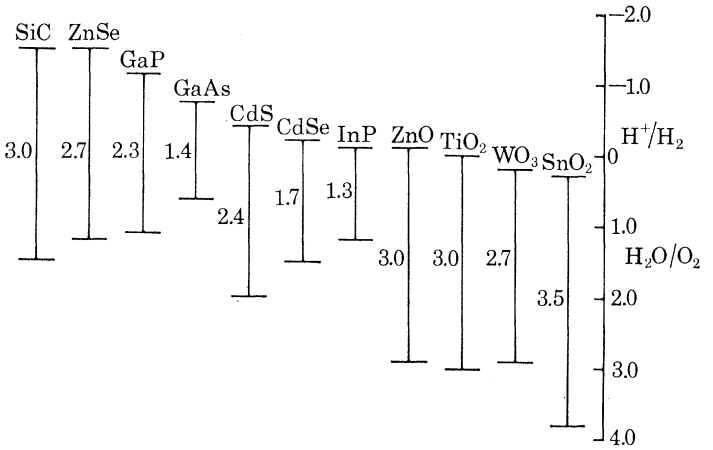

FIGURE 3. Position of valence and conduction band edges for several semiconductors in contact with aqueous electrolyte at pH = 1.0.

The most accurate compilation of experimental flat-band potentials for many semiconductors, measured for both n- and p-type materials at several pH values and accounting for frequency dependent effects, has been presented by Gomes & Cardon (1977); the U_{fb} values are reported to be accurate within 0.05–0.1 V. From the flat-band potential, and a knowledge of the carrier density, the effective mass, and the band gap of the semiconductor, the conduction and valence band edges can be determined with respect to the standard redox scale. These data are presented in figure 3 for several semiconductors at pH = 1.0.

3. ENERGETICS OF PHOTOELECTROCHEMICAL CELLS

(a) *Photo-induced charge transfer reactions*

When the semiconductor–electrolyte junction is illuminated with light, photons having energies greater than the semiconductor band gap are absorbed and create electron–hole pairs in the semiconductor. Photons absorbed in the depletion layer produce electron–hole pairs that separate under the influence of the electric field present in the space charge region. Electron–hole pairs produced by absorption of photons beyond the depletion layer will separate if the minority carriers can diffuse to the depletion layer before recombination with the majority carriers occurs. Photons will be absorbed in the depletion layer if their absorption coefficient, α cm^{-1}, is sufficiently large such that $\alpha^{-1} < w$, where w is the depletion layer width.

The photoproduction and subsequent separation of electron–hole pairs in the depletion layer cause the Fermi level in the semiconductor to return toward its original position before the semiconductor–electrolyte junction was established, i.e. under illumination the semiconductor potential is driven toward its flat-band potential. Under open circuit conditions between an illuminated semiconductor electrode and a metal counter electrode, the photovoltage produced between the electrodes is equal to the difference between the Fermi level in the semiconductor and the redox potential of the electrolyte. Under closed circuit conditions, the Fermi level in the system is equalized and no photovoltage exists between the two electrodes.

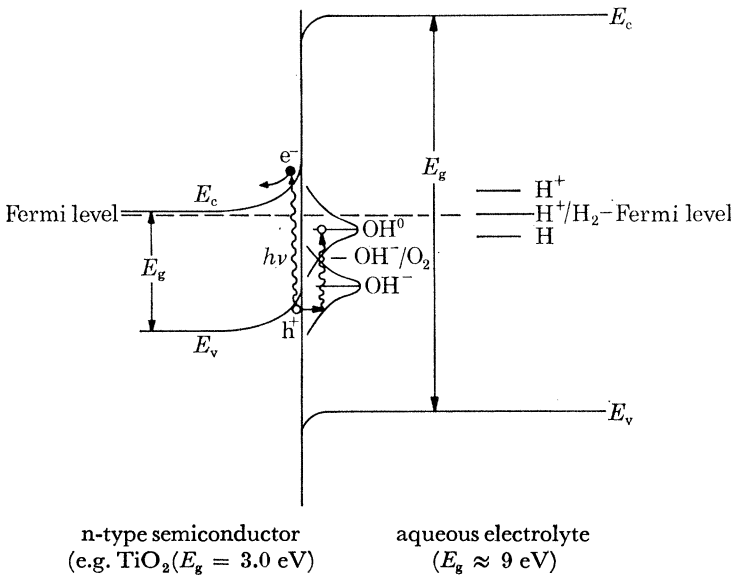

FIGURE 4. Heterojunction model for semiconductor–electrolyte junction in which water is treated like a semiconductor with redox levels represented as extrinsic defect states.

However, a net charge flow does exist. Photogenerated minority carriers in the semiconductor are swept to the surface where they are subsequently injected into the electrolyte to drive a redox reaction. For n-type semiconductors, minority holes are injected to produce an anodic oxidation reaction, while for p-type semiconductors, minority electrons are injected to produce a cathodic reduction reaction. The photo-generated majority carriers in both cases are swept toward the semiconductor bulk, where they subsequently leave the semiconductor via an ohmic contact, traverse an external circuit to the counter electrode, and are then injected at the counter electrode to drive a redox reaction inverse to that occurring at the semiconductor electrode.

Models for the semiconductor–electrolyte junction usually consider the electrolyte as a metal whereby the electrolyte redox potential is analogous to the metal work function. In a new model recently proposed by Williams & Nozik (1978) aqueous electrolyte is considered as a semiconductor (Williams *et al.* 1978), and the semiconductor–electrolyte junction is treated like a heterojunction between two different semiconductors. An energy level diagram for this model is shown in figure 4. The band gap of H_2O is taken as about 9 eV, and its electron affinity is 0.5 eV. Redox couples in the aqueous electrolyte are treated as extrinsic electronic states.

In the heterojunction model, photogenerated minority carriers created in the depletion layer find themselves in an asymmetric potential well (see figure 5). One side of the well has

a parabolic shape with a height equal to the band bending (V_b); the other side is a vertical wall with a height (U) equal to either the difference between the valence band edge of water and the valence band edge of the semiconductor (for n-type semiconductors), or the difference between the conduction band edge of water and the conduction band edge of the semiconductor (for p-type semiconductors). The thickness of the vertical barrier, d, depends upon the distance from the semiconductor surface of the relevant electrolyte species participating in the charge transfer reaction. For absorbed species, this distance is 2–3 Å.

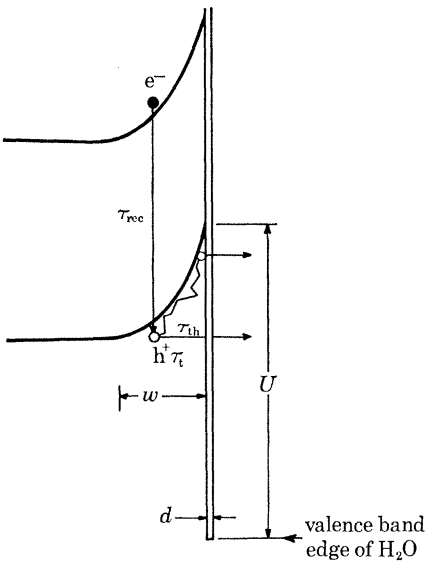

FIGURE 5. Potential well in depletion layer at semiconductor–electrolyte interface for n-type semiconductors.

In this model, charge transfer of photogenerated minority carriers can be considered to proceed via quantum mechanical tunnelling from the potential well of the depletion layer into the electrolyte (Nozik *et al.* 1979; Williams & Nozik 1978). Another aspect of this work is the consideration of the possibility of 'hot carrier' injection across the semiconductor–electrolyte interface.

Hot carrier injection is defined as a process where photogenerated minority carriers are injected into the electrolyte before they undergo complete intra-band relaxation (thermalization) in the semiconductor depletion layer. The total time for thermalization is the time required for minority carriers to dissipate all of the band bending potential energy through carrier-phonon collisions. If the thermalization time is greater than the effective residence time of the minority carriers in the depletion layer, then hot carrier injection can occur. Preliminary calculations (Nozik *et al.* 1979) for n-TiO_2 anodes and p-GaP cathodes indicate that hot carrier injection processes are feasible in these systems. Some recent experimental results (Dickson & Nozik 1978) on the photoreduction of N_2 on p-GaP cathodes provide qualitative evidence for hot carrier injection.

The occurrence of hot carrier injection in photoelectrochemical reactions would be very significant for the following reasons: (1) the nature of the permitted photo-induced reactions at semiconductor electrodes could be controlled by polarization of the electrode; (2) the

photogenerated carriers would not be in thermal equilibrium in their respective bands so that quasi-thermodynamic arguments, such as the use of the quasi-Fermi level to describe the energetics of photoelectrochemical reactions, would not be valid; (3) the influence of surface states would be restricted to the class of states originating from the chemical interaction of the electrolyte with the semiconductor surface; and (4) the maximum theoretical conversion efficiency for photoelectrochemical energy conversion would be different from the case of thermalized injection.

(*b*) *Semiconductor electrode stability*

The photo-generated holes and electrons in semiconductor electrodes are generally characterized by strong oxidizing and reducing potentials, respectively. Instead of being injected into the electrolyte to drive redox reactions, these holes and electrons may oxidize or reduce the semiconductor itself, and cause decomposition. This possibility is a serious problem for practical photoelectrochemical devices, since photodecomposition of the electrode leads to inoperability or to short electrode lifetimes.

A simple model of electrode stability has been presented by Gerischer (1977*b*) and by Bard & Wrighton (1977). The redox potential of the oxidative and reductive decomposition reactions are calculated and put on an energy level diagram like figure 2. The relative positions of the decomposition reactions are compared with those of the semiconductor valence and conduction band edges. Absolute thermodynamic stability of the electrode is assured if the redox potential of the oxidative decomposition reaction of the semiconductor lies below (has a more positive value on the s.c.e. scale) the valence band edge, and if the redox potential of the reductive decomposition reaction lies above (has a more negative value on the s.c.e. scale) the conduction band edge. This situation does not exist in any of the semiconductors studied to date. More typically, one or both of the redox potentials of the semiconductor oxidative and reductive decomposition reactions lie within the band gap, and hence become thermodynamically possible. Electrode stability then depends upon the competition between thermodynamically possible semiconductor decomposition reactions and thermodynamically possible redox reactions in the electrolyte. This competition is governed by the relative kinetics of the two possible types of reactions.

For TiO_2, the redox potential for the oxidation of water to O_2 is more negative than that for the oxidation of TiO_2 to O_2; therefore, the former couple lies further above the valence band edge than the latter couple. This makes the water oxidation reaction more thermodynamically favoured than the TiO_2 oxidation reaction. This means that, at equilibrium, the conversion of water to oxygen would be greater than the conversion of the TiO_2 oxidation reaction. However, equilibrium is generally never attained here, and kinetic factors predominate. It is very difficult to predict kinetic behaviour, and one must rely on experimental data. For TiO_2, it has been found that water oxidation proceeds nearly exclusively rather than TiO_2 oxidative decomposition. However, some evidence of TiO_2 degradation does exist, especially in acidic solutions (Harris & Wilson 1976).

In cases where the redox potentials of the electrode decomposition reactions are more thermodynamically favoured than the electrolyte redox reactions (oxidative decomposition potential more negative, reductive decomposition potential more positive, than the corresponding electrolyte redox reactions), the products of the electrolyte redox reactions have sufficient potential to drive the electrode decomposition reactions. Hence this situation usually results in electrode instability, assuming that the electrode decomposition reaction is not

PHILOSOPHICAL TRANSACTIONS OF THE ROYAL SOCIETY A MATHEMATICAL, PHYSICAL & ENGINEERING SCIENCES

kinetically inhibited. This is the case with ZnO, Cu_2O, and CdS in simple aqueous electrolytes, and these semiconductors are indeed unstable under these conditions.

It appears that the more thermodynamically favoured redox reactions also become kinetically favoured, so that these reactions predominate. This effect has been used to stabilize semiconductor electrodes by establishing a redox couple in the electrolyte with a redox potential more negative than the oxidative decomposition potential (or more positive than the reductive decomposition potential), such that this electrolyte redox reaction occurs preferentially to the decomposition reaction, and scavenges the photo-generated minority carriers (Gerischer 1977*a*; Bard & Wrighton 1977). However, this stabilization technique can only be used for electrochemical photovoltaic cells, and it is discussed later in further detail.

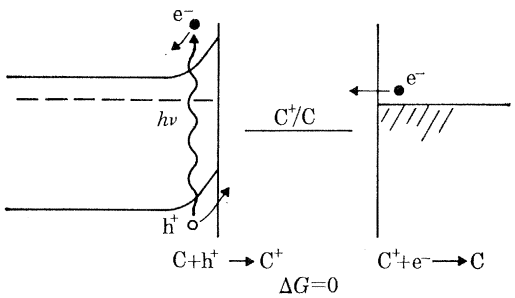

FIGURE 6. Energy level diagram for electrochemical photovoltaic cell. C^+/C is a redox couple in the electrolyte which produces the indicated anodic and cathodic reactions such that no net chemical change occurs.

(*c*) *Electrochemical photovoltaic cells*

An energy level diagram for electrochemical photovoltaic cells is shown in figure 6. One predominant redox couple, represented as C^+/C, is present in the electrolyte such that C is oxidized to C^+ at the anode and C^+ is reduced to C at the cathode. The usual cell configuration comprises one semiconductor electrode and one metal electrode; the semiconductor electrode may be n- or p-type although in practice it is usually always n-type. Hence, in this case, photo-generated holes drive an oxidation reaction at the semiconductor surface while photo-generated electrons are driven into the bulk of the semiconductor, exit at a rear ohmic contact, circulate externally through a load, and then are injected at the metal cathode to produce the reduction reaction. No net chemical change is produced in the electrolyte, and electrical power is delivered to the external load through the photovoltage and photocurrent generated by the semiconductor electrode.

The maximum possible open-circuit photovoltage is equal to the band bending, which is the difference between the flat-band potential of the semiconductor and the redox potential of the predominant redox couple in the electrolyte. The photocurrent depends upon the semiconductor band gap and the quantum efficiency. The relation between the maximum short circuit photocurrent and the band gap has been well established for sunlight (Wolf 1960).

The factors determining the maximum theoretical efficiency for electrochemical photovoltaic cells are completely analogous to those for solid state photovoltaic cells. It is necessary to optimize the product of the external photovoltage and photocurrent, and this is achieved with a semiconductor band gap of about 1.3–1.4 eV. The general principles of the operation of

PHILOSOPHICAL TRANSACTIONS OF THE ROYAL SOCIETY A MATHEMATICAL, PHYSICAL & ENGINEERING SCIENCES

electrochemical photovoltaic cells were presented by Gerischer (1975) and by Anderson & Chai (1976).

For p–n photovoltaic devices, the optimum band gap yields upper limit conversion efficiencies of about 25%. For solid state Schottky photovoltaic cells, the calculated maximum efficiencies are lower for the same semiconductor materials; this is because the potential barrier height (band bending) at the semiconductor–metal junctions are low compared with the semiconductor band gap. The upper limit efficiency for solid state Schottky cells is about 10–12%.

In this regard, electrochemical photovoltaic cells have a major potential advantage, because the band bending may be increased by adjusting the redox potential of the electrolyte. For n-type electrodes a redox couple with a more positive redox potential could be introduced into the electrolyte, while for p-type electrodes more negative redox potentials are required.

Other important advantages of liquid junction photovoltaic cells compared with solid state cells are the great ease with which the liquid junction potential barrier can be established (the semiconductor electrode is simply immersed in the electrolyte), and the fact that polycrystalline semiconductor films can be used without a drastic decrease in efficiency, compared with single crystal semiconductor electrodes. The latter effect is probably due to the intimate and perfect contact of the liquid electrolyte with the crystallite grains, in contrast to the imperfect contact between two solid, polycrystalline phases. The maximization of the band bending by adjustment of the redox potential of the electrolyte is limited by considerations of electrode stability. If the redox potential of the redox couple in the electrolyte is made too positive with n-type electrodes, or too negative with p-type electrodes, then the electrode decomposition reaction may become more thermodynamically and/or kinetically favoured. On the other hand, electrodes that are unstable in a given electrolyte may be stabilized by adding to the electrolyte a redox couple having a redox potential more thermodynamically and/or kinetically favoured compared with the decomposition potential. Thus, electrochemical photovoltaic cells have much greater flexibility with respect to possible solutions to the electrode stability problem than photoelectrolysis cells. For the latter, the redox couples in the electrolyte are fixed by the desired net chemical reaction in the cell, and their redox potentials cannot be adjusted with respect to the potentials of the electrode decomposition reactions. For the former, the redox potentials of the electrolyte redox couples may be adjusted to stabilize the electrode within the constraint of maintaining sufficient band bending, and hence open circuit voltage.

The first demonstration of the principle of electrode stabilization by incorporation into the electrolyte of thermodynamically and/or kinetically favoured redox couples was made with n-CdS electrodes in basic electrolyte containing the sulphide–polysulphide (S^{2-}/S_n^{2-}) redox couple (Ellis *et al.* 1976; Miller & Heller 1976). Conversion efficiencies of 1–2% were reported for this first, stable liquid junction solar cell.

Studies have been made of other cadmium chalcogenide electrodes (CdSe, CdTe) in polychalcogenide electrolytes (S^{2-}/S_n^{2-}, Se^{2-}/Se_2^{2-}, Te^{2-}/Te_2^{2-}). For the nine cadmium chalcogenide electrode–polychalcogenide electrolyte combinations, only CdTe with S^{2-}/S_n^{2-} was found to be grossly unstable (Ellis *et al.* 1977). Heller *et al.* (1977) reported 8% conversion efficiency in natural sunlight with CdSe and CdTe electrodes in polychalcogenide electrolyte. A comparison by Miller *et al.* (1977) of single crystal and polycrystalline (pressure sintered) CdSe showed the conversion efficiency of the latter system to be 5.1% compared with 7.5% for the former system.

Several III–V semiconductor electrodes (GaAs, GaP and InP) have also been studied with

PHILOSOPHICAL TRANSACTIONS OF THE ROYAL SOCIETY A MATHEMATICAL, PHYSICAL & ENGINEERING SCIENCES

polychalcogenide electrolytes (Ellis *et al.* 1977*b*; Chang *et al.* 1977). The highest efficiency for any liquid junction solar cell (12%) has been reported (Parkinson *et al.* 1978) for n-GaAs in polyselenide electrolyte using carbon cathodes.

In addition to the II–VI and III–V semiconductor electrodes discussed above, other interesting semiconductors have been examined in electrochemical photovoltaic cells. Legg *et al.* (1977) have reported that n-Si can be stabilized by using a nonaqueous electrolyte containing the ferricenium/ferrocene redox couple $(Fe/Cp)_2^-/Fe(Cp)_2$). Wrighton *et al.* (1978) have shown that ferrocene derivatives can be bonded directly to the Si surface and produce stabilization of the surface. Furthermore, these modified electrode surfaces exhibit mediated electron transfer reactions. These results are very significant as they point to a new method for electrode stabilization and Si is the primary material under development for economical solid state solar cells.

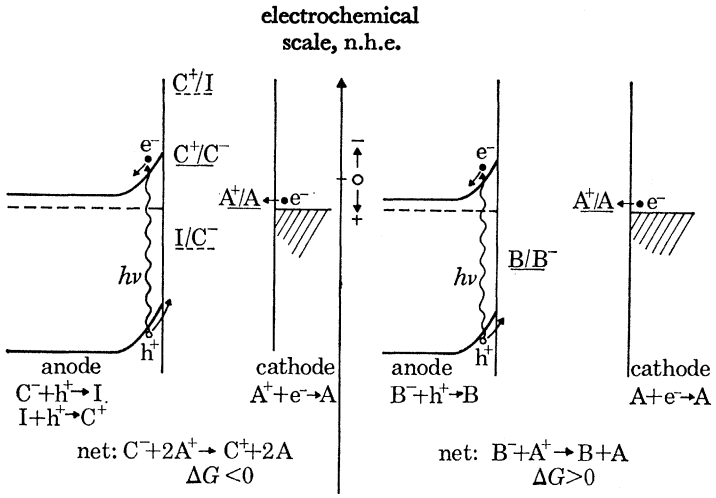

FIGURE 7. Energy level diagrams for photoelectrolysis cells (right) and photocatalytic cells (left). A^+/A, B/B^-, and C^+/C^- are generalized redox couples; I/C and C^+/I are redox couples for intermediate steps of the C^+/C^- couple.

A new class of electrode materials has been proposed by Tributsch (1977). Here, stability is produced by having the optical transition in the semiconductor occur between energy bands formed from the d-orbitals of the metal component rather than between an anion-like valence band and a cation-like conduction band. This situation exists in metal dichalcogenides (such as MoS_2 and WS_2) where the top of the valence band is derived from $4d_z2$ orbitals and the conduction band is derived from $4d_{xy}$ and $4d_x2_y2$ orbitals. Thus, absorption of light and the creation of electron-hole pairs is not expected to produce a rupture of the bonding between anions and cations. Initial experiments with MoS_2 showed that while the sulphide ion in the crystal was stabilized against direct oxidation by photo-generated holes, the crystal itself was unstable with respect to the oxidation product of the electrolyte (O_2), and sulphates were produced, which caused electrode instability.

(*d*) *Photoelectrosynthetic cells*

Energy level diagrams for the two types of photoelectrosynthetic cells are presented in figure 7.

(i) *Photoelectrolysis cells*

In photoelectrolysis cells, the anodic reaction has a more positive redox potential than the cathodic reaction so that the overall cell reaction has a positive free energy change.

Two types of photoelectrolysis cells can be distinguished. In the first type, one electrode is a semiconductor and the second a metal. In the second type, one electrode is an n-type semiconductor and the second a p-type semiconductor. The energetics of the former cell is represented in figure 8 for the photoelectrolysis of water into H_2 and O_2 by using n-type electrodes

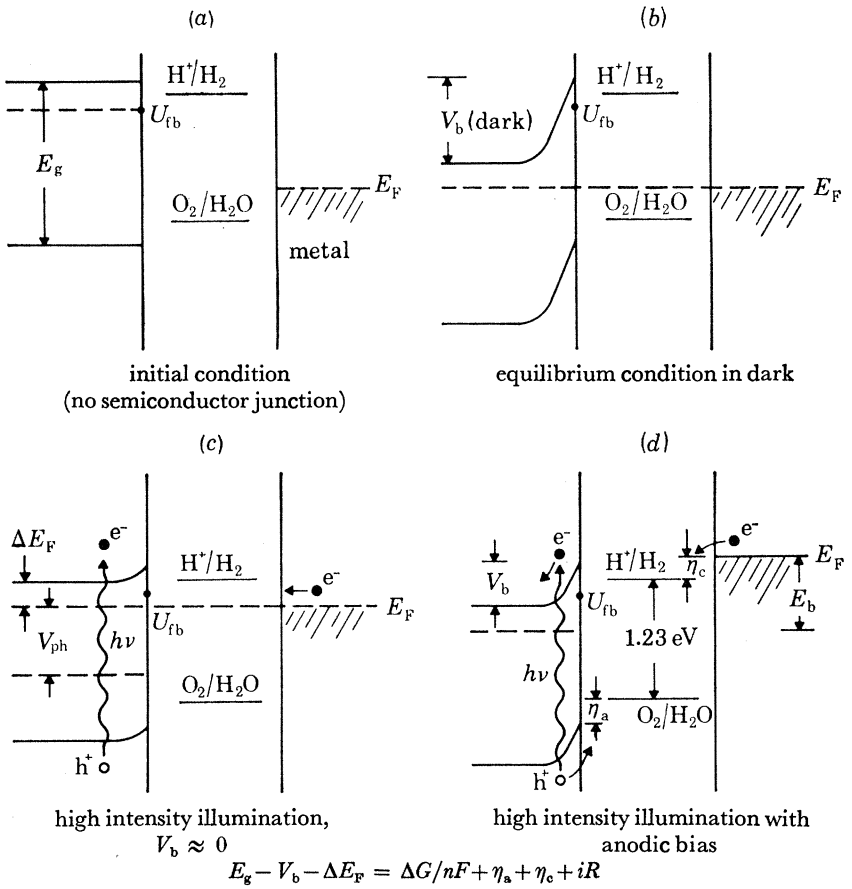

FIGURE 8. Sequence of energy level diagrams for a single semiconductor electrode photoelectrolysis cell from the initial condition to the final condition of photoelectrolysis with bias. Energy balance is written for case of zero bias; if bias is present, E_b is added to left side of equation.

(analogous analyses apply to p-type electrodes). Since there are two redox couples in the electrolyte, the initial Fermi level in the electrolyte can be anywhere between them depending upon the initial relative concentrations of H_2 and O_2 in the cell. In figure 8*a* the initial Fermi level in the electrolyte is arbitrarily drawn just above the O_2–H_2O redox level. Upon equilibration in the dark (figure 8*b*), the Fermi level in the semiconductor equilibrates with the electrolyte Fermi level producing a band bending, V_b in accordance with equation (1).

Under illumination (figure 8*c*), the Fermi level in the semiconductor rises toward U_{fb} producing a photovoltage, V_{ph}. This voltage can be measured between the two electrodes with an external potentiometer. However, the value of V_{ph} depends upon the initial metal electrode

potential, which depends upon the initial relative concentrations of H_2 and O_2: V_{ph} can vary from zero to some finite value. Except under very special circumstances (initial metal electrode potential and the valence band edge of the semiconductor electrode both at the O_2/H_2O redox potential), V_{ph} is not the potential energy available for photoelectrolysis.

With the two electrodes shortened together, the maximum Fermi level possible in the cell is the flat-band potential. In figure 8 U_{fb} is below the H^+/H_2 redox potential. Hence, even with illumination intensity sufficient to completely flatten the semiconductor bands, H_2 could not be evolved at the counter electrode because the Fermi level is below the H^+/H_2 potential (figure 8*c*). In order to raise the Fermi level in the metal counter electrode above the H^+/H_2 potential, an external anodic bias, E_b, must be applied, as shown in figure 8*d*. This bias also provides the overvoltage at the metal cathode, η_c, required to sustain the current flow, and it increases the band bending in the semiconductor to maintain the required charge separation rate.

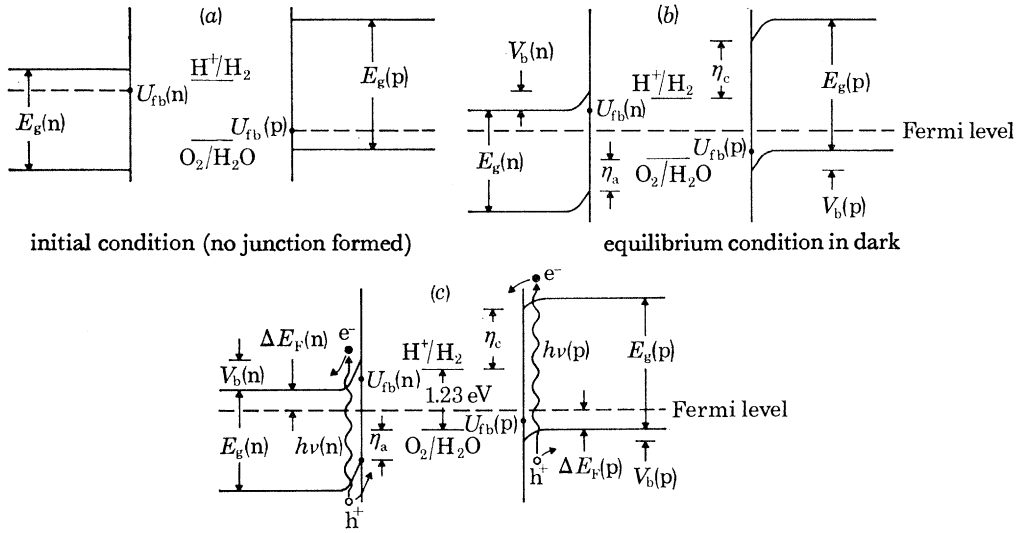

$$E_g(h) + E_g(p) - (U_{fb}(p) - U_{fb}(h)) + \Delta E_F(h) - \Delta E_F(p) = \Delta G/nF + \eta_a + \eta_c + iR$$

FIGURE 9. Sequence of energy level diagrams for double electrode photoelectrolysis cell.

The situation depicted in figure 8 is the one that describes most of the n-type semiconductors studied to date. For these semiconductors, an external bias is required to generate H_2 and O_2 in a Schottky-type photoelectrolysis cell; the further U_{fb} lies below H^-/H_2, the greater the bias. The bias can be applied either by an external voltage source or by immersing the anode in base and the cathode in acid (the two compartments being separated by a membrane).

Several semiconductors such as $SrTiO_3$, $KTaO_3$, Nb_2O_5 and ZrO_2 have U_{fb} above the H^+/H_2 potential: therefore, no external bias is required to generate H_2 and O_2 in a Schottky type cell. This has been confirmed for $SrTiO_3$ and $KTaO_3$. Unfortunately, these oxides all have large band gaps (3.4–3.5 eV), which result in essentially zero solar absorptivity, and hence they are ineffective in systems for solar energy conversion.

For purposes of discussion of figure 8, the difference between the O_2/H_2O redox potential and the valence band edge at the interface is defined as the intrinsic overpotential of the semiconductor anode, η_a. This overpotential is not the usual overpotential or overvoltage of conventional electrochemistry since it is current independent and is determined only by the band gap, the flat-band potential, and the redox potential of the electrolyte donor state.

A simple identity can be derived from the energy diagram of figure 8*d* and it is given at the bottom of figure 8. This identity can be considered to represent an energy balance describing the distribution of the energy produced by the absorption of a photon by the semiconductor. In the absence of a bias, the input energy of an absorbed photon is equal to the semiconductor band gap. Energy loss terms in the semiconductor resulting from the movement of electrons and holes from their point of creation to the respective electrolyte interfaces are the band bending (V_b), and the difference between the conduction band edge in the bulk and the Fermi level (ΔE_F). The net electron-hole pair potential available at the electrode interfaces is thus $E_g - V_b - \Delta E_F$. In the electrolyte, a portion of this potential energy is recovered as the free energy ($\Delta G/nF$) of the net endoergic reaction in the electrolyte. The rest of the potential energy is lost through the irreversible, entropy-producing terms η_a, η_c, and iR (ohmic heating).

For the case where both electrodes are n and p-type semiconductors, the most interesting situation occurs when the two electrodes are made of different semiconductors. If the electron affinity of the n-type electrode is greater than that of the p-type electrode, then the available electron-hole potential for driving chemical reactions in the electrolyte is enhanced when both electrodes are illuminated. The energetics of this system is shown in figure 9.

As seen from the energy balance presented at the bottom of figure 9, the net electron–hole pair potential available at the electrode surfaces is the sum of the semiconductor band gaps minus the difference in their flat-band potentials and minus the Fermi level terms, ΔE_F, for each semiconductor. The sum of the band bending values produced at each semiconductor is equal to the difference between their flat-band potentials. The amount of potential enhancement is maximized if the difference in flat-band potentials is minimized. The minimum difference in flat-band potentials is determined by the minimum band bending required in each semiconductor electrode to produce efficient charge carrier separation. The total band bending present in the two electrodes is independent of light intensity. However, the distribution of the total band bending between the electrodes is dependent upon light intensity and the carrier densities of each electrode.

In the cell, two photons must be absorbed (one in each electrode) to produce one net electron–hole pair for the cell reaction. This electron–hole pair consists of the minority hole and minority electron from the n-type and p-type electrodes, respectively, and it has a potential energy greater than that available from the absorption of one photon. The majority electrons and holes recombine at the ohmic contacts.

An important possible advantage of the double electrode cell is that for a given cell reaction it may allow the use of smaller band gap semiconductors. Since the maximum photocurrent available from sunlight increases rapidly with decreasing band gap, this could produce higher conversion efficiencies. For the splitting of water into H_2 and O_2 with sunlight, the maximum theoretical efficiency has been estimated to be about 25% (Nozik 1977*a*). This is to be compared to the value of about 16% for the maximum efficiency of water splitting by a photovoltaic cell in series with a conventional electrolysis cell.

(ii) *Photochemical diodes*

The enhanced electron–hole potential available from double semiconductor electrode cells can eliminate the bias required for single semiconductor electrode cells when V_{fb} is below the H^+/H_2 redox potential. This was shown for the first time (Nozik 1976; Yoneyama *et al.* 1975)

PHILOSOPHICAL TRANSACTIONS OF THE ROYAL SOCIETY A MATHEMATICAL, PHYSICAL & ENGINEERING SCIENCES

with an n-TiO_2/p-GaP cell; photoelectrolysis of water into H_2 and O_2 was achieved at zero external bias with simulated sunlight (Nozik 1977*b*).

Further studies have been made with n-TiO_2/p-CdTe, n-$SrTiO_3$/p-CdTe, and n-$SrTiO_3$/p-GaP cells (Ohashi *et al.* 1977).

The elimination of bias requirements for photoelectrolysis cells through the use of double electrode systems leads to a very interesting configurational variation. This configuration has been labelled 'photochemical diodes' (Nozik 1977*b*), and comprises photoelectrolysis cells that are collapsed into monolithic particles containing no external wires. In one simple form photochemical diodes consist of a sandwich or either a semiconductor and a metal, or an n-type and a p-type semiconductor, connected together through ohmic contacts.

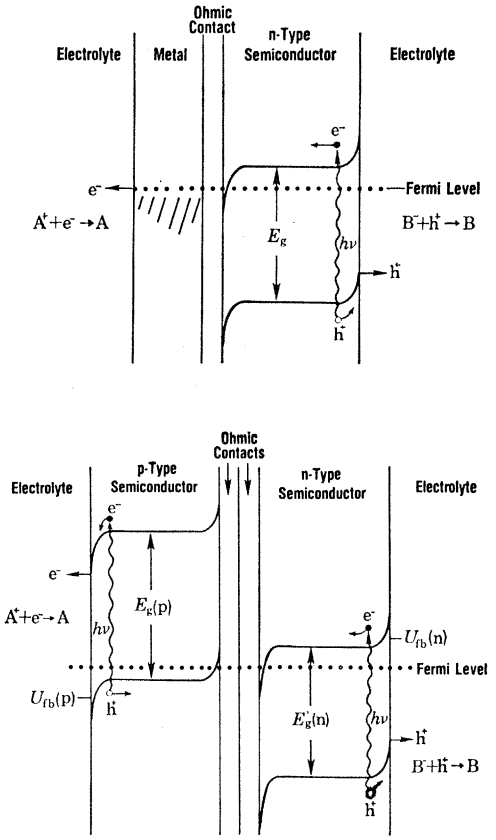

FIGURE 10. Energy level diagrams for photochemical diodes. Top, single semiconductor–metal (Schottky) type photochemical diode; bottom, double semiconductor (p–n) type photochemical diode (n and p-type semiconductors). A two photon process with voltage enhancement is produced in the latter.

To generate the relevant redox reactions, photochemical diodes are simply immersed in an appropriate electrolyte, and the semiconductor faces illuminated. An energy level diagram for photochemical diodes consisting of heterotype p- and n-type electrodes is shown in figure 10. A comparison of this energy level scheme with that for biological photosynthesis reveals very interesting analogies (see figure 11). Both systems require the absorption of two photons to produce one useful electron–hole pair. The potential energy of this electron–hole pair is enhanced so that chemical reactions requiring energies greater than that available from one photon can be driven. Furthermore, the n-type semiconductor is analogous to Photosystem II,

the p-type semiconductor is analogous to Photosystem I, and the recombination of majority carriers at the ohmic contacts is analogous to the recombination of the excited electron from Excited Pigment II with the photo-generated hole in Photosystem I (Nozik 1977).

The size of a photochemical diode is arbitrary, provided that there is sufficient optical absorption, and a space charge layer exists that is consistent with efficient charge carrier separation. Within these constraints, the particle size may approach colloidal, or perhaps macromolecular dimensions, and the diodes may possibly operate as a colloidal dispersion or as a solute in solution, thereby greatly simplifying the design and operation of photoelectrochemical reactors using sunlight.

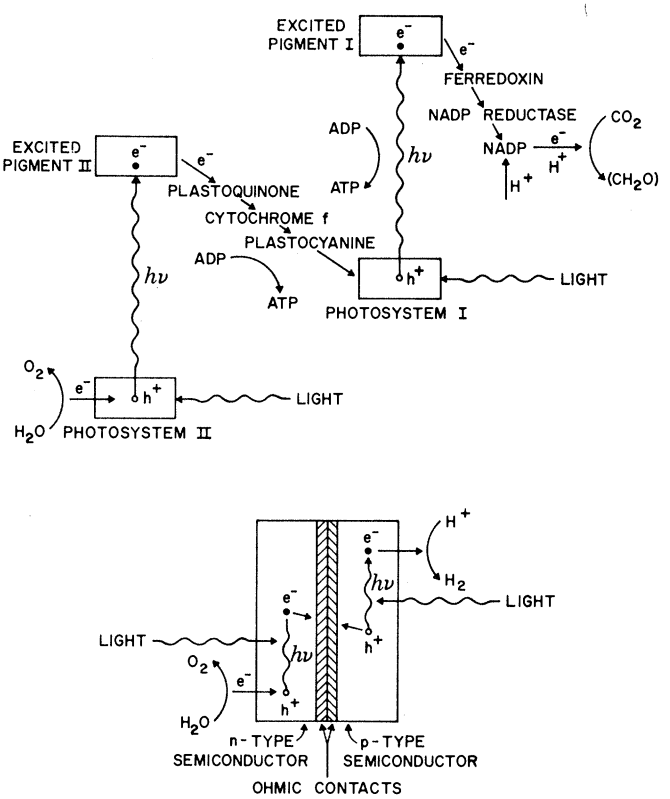

FIGURE 11. Comparison of the electron flow in biological photosynthesis with that in the double semiconductor-type photochemical diode. In both cases, two separate photosystems are involved with subsequent enhancement of the available electron–hole potential.

Kraeutler & Bard (1978*a*) have made studies of powdered semiconductors which were platinized and used as photocatalysts to decompose carboxylic acids to alkanes, hydrogen and carbon dioxide. These platinized semiconductor powders were also used to drive other photoreactions, such as the oxidation of CN^- to OCN^- (Bard 1978). The platinization of semiconductor powders is a method for producing semiconductor-metal type photochemical diodes having the energy level scheme shown in figure 10 (top). However, the reactions studied by Kraeutler & Bard (1978*b*) are exoergic, and hence are considered later in the subsection on photocatalysis.

More than two dozen semiconductors have been studied as electrodes (Nozik 1978), and the highest conversion efficiency obtained for water splitting in a stable photoelectrolysis cell is between 0.5 and 1.0%. Most of the semiconductors studied to date have been n-type oxides,

since oxides are generally more stable against photoelectrochemical oxidation than nonoxides. Semiconductor oxides that operate with zero bias in a single electrode cell (U_{fb} above the H^+/H_2 level) generally have large band gaps ($E_g > 3$ eV), such as $SrTiO_3$, $KTaO_3$, Ta_2O_5, and ZrO_2. Smaller band gap oxides or non-oxides studied thus far are generally either unstable or require a significant external bias.

A few p-type materials have been examined as cathodes for photoelectrolysis cells (e.g. p-GaP, p-InP, p-CuO, p-CdTe, p-ZnTe, p-GaAs, and p-Si). The relative stability of p-type semiconductors against reductive decomposition is generally greater than the stability of n-type semiconductors against oxidative decomposition. Even non-oxide semiconductors with small band gaps, such as p-Si and p-GaP, appear to be stable when used as cathodes. However, the flat-band potentials of these materials with respect to the H_2O–O_2 redox level are unfavourable, and large bias voltages must be applied.

(iii) *Photocatalytic cells*

Photocatalytic cells are defined as those cells wherein the overall cell reaction has a negative free energy change, but the reaction only proceeds at significant rates under the influence of light.

The energy level diagram for photocatalytic cells is shown in the left side of figure 7. The standard redox potential of the net cathodic reaction is more positive than that of the net anodic reaction, and the overall cell reaction is thus thermodynamically favoured. However, the first step of the anodic reaction (represented as $C^- + h^+ \rightarrow I$ in figure 6) may have a redox potential more positive than the cathodic reaction, and the overall anodic reaction will not proceed in the dark. However, illumination of the anode and the creation of holes with a large positive redox potential (figure 7) can drive the energetic first step of the anodic reaction. Thus, the light effectively provides the activation energy for the overall cell reaction.

Several examples of photocatalysis in photoelectrochemical cells have been demonstrated to date. These examples involve both separated electrode configurations and particulate systems (i.e. photochemical diodes). Dickson & Nozik (1978) have shown that N_2 can be photocatalytically reduced with Al by using a single crystal p-GaP cathode and an aluminium metal anode. Krauetler & Bard (1978), using platinized n-TiO_2 powders, have shown that carboxylic acids can be oxidized to CO_2 and alkanes, and that CN^- can be oxidized to OCN^-. Undoubtedly, additional interesting and significant photocatalytic reactions and systems will be discovered in the future.

4. Summary

Three types of photoelectrochemical cells have been described: electrochemical photovoltaic cells, photoelectrolysis cells, and photocatalytic cells. In the first type, optical energy is converted into electrical energy; in the second type, optical energy is converted into chemical energy; and in the third type, optical energy provides the activation energy for exoergic reactions.

Critical semiconductor electrode parameters for these systems are the flat-band potential and the band gap. The latter governs the absorption characteristics and hence the ultimate conversion efficiency possible in the cells; the former establishes the maximum attainable photovoltage from electrochemical photovoltaic cells, the external bias requirements for photoelectrolysis cells, and the permitted range of redox reactions for photocatalytic cells.

PHILOSOPHICAL TRANSACTIONS OF THE ROYAL SOCIETY A MATHEMATICAL, PHYSICAL & ENGINEERING SCIENCES

Electrode stability is a major problem for photoelectrochemical devices. For photoelectrolysis cells, n-type semiconductors that are stable against oxidative decomposition during O_2 evolution are limited thus far to wide band gap oxides ($E_g > 2.2$ eV), and this results in low conversion efficiency (maximum reported values with sunlight are about 0.5–1.0%). Smaller band gap p-type semiconductors appear to be stable against reductive decomposition, but large external bias voltages are required for photoelectrolysis. For electrochemical photovoltaic cells, relatively good electrode stability has been achieved with low band gap semiconductors (Si, GaAs, CdX, X = S, Se, Te) by establishing a redox couple in the electrolyte that is thermodynamically and/or kinetically favoured over the electrode decomposition reaction. Conversion efficiencies as high as 12% have been reported with such cells.

A new and interesting configuration for photoelectrosynthetic cells, comprising monolithic structures containing no external wires, has been demonstrated and named 'photochemical diodes'. These photochemical diodes can be in powder form and simply suspended in electrolyte and illuminated to drive the electrolyte reactions.

A rigorous and detailed theory for photoelectrolysis has not yet been derived, and controversy exists concerning the energetics, mechanism, and upper limit conversion efficiency for photoelectrolysis. However, it is generally accepted that for the splitting of water into H_2 and O_2 by using sunlight, the maximum possible efficiency for an optimum photoelectrolysis cell is significantly greater than that obtained with an optimum solar cell (solid state or liquid junction) in series with a conventional electrolysis cell.

The major advantages of photoelectrochemical devices are the great ease with which the semiconductor–electrolyte junction is formed (the semiconductor is simply immersed into the electrolyte) and that the fact that thin, polycrystalline, semiconductor films can be used without serious loss of conversion efficiency compared to single crystal semiconductors.

Although significant advances have been made, both in the basic understanding of photoelectrochemical devices and in the development of systems with good conversion efficiency and stability, much additional research and development must be done before photoelectrochemical systems can be seriously considered for practical solar energy conversion schemes.

References (Nozik)

Anderson, W. W. & Chai, Y. G. 1976 *Energy Convers.* **15**, 85.

Bard, A. J. 1978 *Proceedings of the 2nd International Conference on the Photochemical Conversion and Storage of Solar Energy*, to be published in *J. Photochem.* January, 1979.

Bard, A. J. & Wrighton, M. S. 1977 *J. electrochem. Soc.* **124**, 1706.

Chang, K. C., Heller, A., Schwartz, B., Menezes, S. & Miller, B. 1977 *Science, N.Y.* **196**, 1097.

Dickson, C. R. & Nozik, A. J. 1978 *J. Am. chem. Soc.* **100**, 8007.

Ellis, A. B., Kaiser, S. W. & Wrighton, M. S. 1976 *J. Am. chem. Soc.* **98**, 1635.

Ellis, A. B., Kaiser, S. W., Bolts, J. M. & Wrighton, M. S. 1977*a* *J. Am. chem. Soc.* **99**, 2839.

Ellis, A. B., Bolts, J. M., Kaiser, S. W. & Wrighton, M. S. 1977*b* *J. Am. chem. Soc.* **99**, 2848.

Fujishima, I. & Honda, K. 1972 *Nature, Lond.* **238**, 37.

Gerischer, H. 1975 *Electroanal. Chem. Interfac. Electrochem.* **58**, 263.

Gerischer, H. 1977*a* *Solar power and fuels* (ed. J. R. Bolton). New York: Academic Press.

Gerischer, H. 1977*b* *J. electroanal. Chem.* **82**, 133.

Gomes, W. P. & Cardon, F. 1977 *Proc. of Conf. on Electrochemistry and Physics of Semiconductor-liquid Interfaces Under Illumination* (ed. A. Heller). Princeton: Electrochemical Society.

Harris, L. A. & Wilson, R. H. 1976 *J. electrochem. Soc.* **123**, 1010.

Harris, L. A. & Wilson, R. H. 1978 *A. Rev. Mater. Sci.* **8**, 99.

Heller, A., Chang, K. C. & Miller, B. 1977 *J. electrochem. Soc.* **124**, 697.

Kraeutler, B. & Bard, A. J. 1978*a* *J. Am. chem. Soc.* **100**, 2239.

PHILOSOPHICAL TRANSACTIONS OF THE ROYAL SOCIETY A MATHEMATICAL, PHYSICAL & ENGINEERING SCIENCES

Kraeutler, B. & Bard, A. J. 1978*b* *J. Am. Chem. Soc.* **100**, 4317.
Legg, K. D., Ellis, A. B., Bolts, J. M. & Wrighton, M. S. 1977 *Proc. natn Acad. Sci. U.S.A.* **74**, 4116.
Lohmann, F. 1967 *Z. Naturf.* A **22**, 843.
Maruska, H. P. & Ghosh, A. K. 1978 *Sol. Energy* **20**, 443.
Miller, B. & Heller, A. 1976 *Nature, Lond.* **262**, 680.
Miller, B., Heller, A., Robbins, M., Menezes, S., Chang, K. C. & Thomson, J. 1977 *J. electrochem. Soc.* **124**, 1019.
Nozik, A. J. 1976 *Appl. Phys. Lett.* **29**, 150.
Nozik, A. J. 1977*a* *Proceedings of Conf. on Electrochemistry and Physics of Semiconductor–liquid Interfaces Under Illumination* (ed. A. Heller). Princeton: Electrochemical Society.
Nozik, A. J. 1977*b* *Appl. Phys. Lett.* **30**, 567.
Nozik, A. J. 1978 *A. Rev. phys. Chem.* **29**, 189.
Nozik, A. J., Boudreaux, D. S., Chance, R. R. & Williams, F. 1979 *Adv. Chem. Ser.* **184**. (In the press.)
Ohashi, K., McCann, J. & Bochris, J. 1977 *Nature, Lond.* **266**, 210.
Parkinson, B. A., Heller, A. & Miller, B. 1978 *Appl. Phys. Lett.* **33**, 521.
Tributsch, H. 1977 *Ber. Bunsenges. phys. Chem.* **81**, 361.
Tributsch, H. & Bennett, J. C. 1977*b* *J. electroanal. Chem.* **81**, 97.
Williams, F. & Nozik, A. J. 1978 *Nature, Lond.* **271**, 137.
Williams, F., Varma, S. & Hillenius, S. 1976 *J. chem. Phys.* **64**, 1549.
Wolf, M. 1960 *Proc. I.R.E.* **48**, 1246.
Wrighton, M., Austin, R. G., Bocarsly, A. B., Bolts, J. M., Haas, O., Legg, K. D., Nadjo, L. & Palazzotto, M. C. 1978 *J. Am. Chem. Soc.* **100**, 1602.
Wrighton, M. 1977 *Technology Review* (*M.I.T.*) **79**, 30.
Yoneyama, H., Sakamoto, H. & Tamura, H. 1975 *Electrochim. Acta* **20**, 341.

PHILOSOPHICAL TRANSACTIONS OF THE ROYAL SOCIETY A MATHEMATICAL, PHYSICAL & ENGINEERING SCIENCES